GEOPHYSICS, VOL. 64, NO. 6 (NOVEMBER-DECEMBER 1999); P. 1748–1755, 7 FIGS., 1 TABLE.

Stacked global satellite gravity profiles

Mara M. Yale* and D. T. Sandwell‡

ABSTRACT

Gravity field recovery from satellite altimetry provides global marine coverage but lacks the accuracy and resolution needed for many exploration geophysics studies. The repeating ground tracks of the ERS-1/2, Geosat, and Topex/Poseidon altimeters offer the possibility of improving the accuracy and resolution of gravity anomalies along widely spaced (~40-km spacing) tracks. However, complete ocean coverage is usually needed to convert the sea-surface height (or along-track slope) measurements into gravity anomalies. Here we develop and test a method for constructing stacked gravity profiles by using a published global gravity grid (Sandwell and Smith, 1997), V7.2, as a reference model for the slope-to-gravity anomaly conversion. The method is applied to stacks (averages) of Geosat/ERM (up to 62 cycles), ERS-1/2 (up to 43 cycles), and Topex (up to 142 cycles) satellite altimeter profiles. We assess the accuracies of the ERS-1/2 profiles through a comparison with a gravity model of the northern Gulf of Mexico (profiles provided by EDCON Inc.). The 40 ERS profiles evaluated have a mean rms difference of 3.77 mGal and full wavelength resolution (0.5 coherence) of 24 km. Our processing retains wavelengths as short as 10 km so smaller, large-amplitude features can be resolved, especially in shallow ocean areas (<1000 m deep). We provide an example of combining these higher resolution profiles with lower resolution gravity data in the Caspian Sea.

INTRODUCTION

Satellite altimetry has provided marine gravity field (or geoid height) globally at wavelengths greater than about 25 km (Cazenave et al., 1996; Hwang and Parsons, 1996; Rapp and Yi, 1997; Sandwell and Smith, 1997; Andersen and Knudsen, 1998). A recent global gravity grid (Sandwell and Smith, 1997), V7.2, was created by combining data from the Geosat and ERS-1 satellites. Each satellite operated in two modes: a geodetic mode, covering the Earth with closely spaced ground tracks (Geosat, 6 km; ERS-1, 8 km), and a repeat mode, covering the Earth many times with more sparsely spaced ground tracks. The repeat mode allows for stacking or averaging profiles, which improves along-track resolution over individual profiles (Yale et al., 1995). While the resolution of the repeat mode data is potentially higher than the geodetic mode data, the V7.2 gravity grid was filtered in two dimensions with a latitude-dependent filter that reflected the average quality and orientation of the geodetic mode data. Thus, the full potential of the repeat-cycle mode data was lost while creating the V7.2 grid with its 2-minute grid spacing.

In this study we recover the full resolution of the repeat mode profile data while remaining compatible with the V7.2 global gravity grid at long wavelengths. We follow the approach of Small and Sandwell (1992) for creating along-track gravity anomalies. After stacking (averaging) along-track sea-surface slopes, the along-track slopes of the V7.2 grid are subtracted, leaving a low-amplitude, short-wavelength structure. Residual sea-surface slopes are converted to gravity anomalies through a 1-D Hilbert transform. Finally, the V7.2 gravity is added to the residual gravity profile to form a full-bandwidth profile that exactly matches the V7.2 grid at long wavelengths. The method is implemented on global data sets of stacked profiles from ERS-1/2, Geosat, and Topex. (We treat ERS-1 and ERS-2 as a single satellite data series since the two satellites have similar characteristics.) Compared with our previous study (Yale et al., 1995), there are now many more cycles of ERS-1/2 and Topex available for stacking; this is especially important for editing outliers and suppressing noise in the ERS-1/2 data.

PROCESSING GLOBAL SATELLITE ALTIMETRY DATA

All three data sets were edited and preprocessed using previously developed methods (Yale et al., 1995; Sandwell and Smith, 1997). Since ERS-1/2 data generally are noisier than Geosat or Topex data, stacking more ERS profiles provides

Manuscript received by the Editor May 11, 1998; revised manuscript received April 30, 1999. Published on Geophysics Online, July 19, 1999.
*Formerly Earth Sciences Group, ERIM International, P.O. Box 134008, Ann Arbor, Michigan 48113-4008; presently The MathWorks, Inc., 3 Apple Hill Drive, Natick, Massachusetts 01760-2098. E-mail: myale@mathworks.com.
‡Cecil H. and Ida M. Green Institute of Geophysics and Planetary Physics, Scripps Institution of Oceanography, University of California, San Diego, La Jolla, California 92093-0225. E-mail: dsandwell@ucsd.edu.

a greater improvement over the other satellites. Moreover, the relatively long repeat cycle of ERS-1/2 (35 days) yields the most dense track spacing of the three repeat orbits. The ERS-1/2 data were restacked using all available cycles (43). At the time of the Yale et al. (1995) resolution analysis, we had only 16 cycles of ERS-1 data. (Since then, ERS-1 has collected much more data and a second satellite, ERS-2, was launched in April 1995. ERS-2 and ERS-1 operated simultaneously in a tandem mission, repeating the same ground track one day apart.) For this study we used 28 cycles of ERS-1 data and 15 cycles of ERS-2 data. For all ERS data, we incorporated the most recent orbits calculated by the Delft Institute for Earth-Oriented Space Research. These orbits are based on their new gravity model, DGM-E04, which provides orbits with a radial precision of 5 cm (Scharroo and Visser, 1998). Similarly, we restacked all of the available Topex 10-day repeat-cycle data (142 cycles) using cycles 1–156 from September 22, 1992, to December 18, 1996. Poseidon-only cycles were excluded, and cycle 118 of Topex data was not acquired. Since the time of our earlier study, the quantity and quality of the Geosat/ERM profiles has not changed, so we used the original stacks (Yale et al., 1995) with up to 62 cycles.

In a previous study of ERS-1 data, we found that rms deviation from the stack increases substantially when the significant wave height (SWH) exceeds about 6 m (Yale et al., 1995). We reanalyzed the SWH for ERS-1/2 data using our more robustly determined stack and reached the same conclusion to edit ERS data with an SWH greater than 6 m. This cutoff eliminates <0.9% of the ERS data, which on average deviate by >15 μrad (i.e., 15 mGal) from the stack.

After stacking the vertical deflections, we applied a post-stack, low-pass Parks–McClellan filter with a gain of 0.9 at a 20-km wavelength and a 0.5 gain at a 10-km wavelength. This eliminates noise while preserving the shortest possible wavelength signals. As shown by Yale et al. (1995), the power of the noise falls off approximately linearly with the number of cycles stacked. Maps of the number of cycles stacked for all three satellites are presented in Figure 1. The ERS stacks now have approximately 40 cycles globally, which compares well with Geosat stacks. Topex stacks have more than 100 cycles globally, and the noise in these profiles will be the smallest of the three satellite orbits. However, the large track spacing makes the Topex tracks less useful for gridding than ERS and Geosat profiles.

After creating the new stacked profiles, residual along-track vertical deflection profiles were constructed by subtracting the along-track vertical deflections from the V7.2 grids (Sandwell and Smith, 1997). These were then converted to residual gravity anomaly (Appendix A). The procedure is similar to that used by Small and Sandwell (1992); however, instead of subtracting only a spherical harmonic model of the vertical deflection, we subtract the vertical deflections used to make the V7.2 gravity grid. The residual now consists of short-wavelength (<30 km), low-amplitude anomalies. An along-track editing procedure was used to eliminate outliers (>30 μrad) from the residual profile. This was especially important near the ends of the residual profiles where the number of profiles available for stacking was low. Finally, we performed the 1-D Hilbert transform (Appendix A) to convert residual vertical deflection to residual gravity and added this to the gravity profile from the V7.2 grid. The 1-D approximation assumes that gravity is lineated perpendicular to ground tracks. When this is not true, the gravity is underpredicted by the 1-D approximation. Our method of applying the 1-D transformation only to residual differences between stacked profiles and V7.2 profiles minimizes the impact of this limitation.

After processing, global gravity anomaly profiles can be treated as shipborne or airborne anomaly profiles, although—unlike shipborne data—they do not contain significant crossover errors. Since their long wavelengths are inherited from the JGM-3 global gravity model developed by Nerem et al. (1994), we believe they provide the best global reference profiles for marine gravity work. Like other types of gravity profiles, each satellite-derived gravity profile can be examined for outliers and combined with available shipboard profiles and other data (e.g., V7.2 grid) to create grids having optimal characteristics.

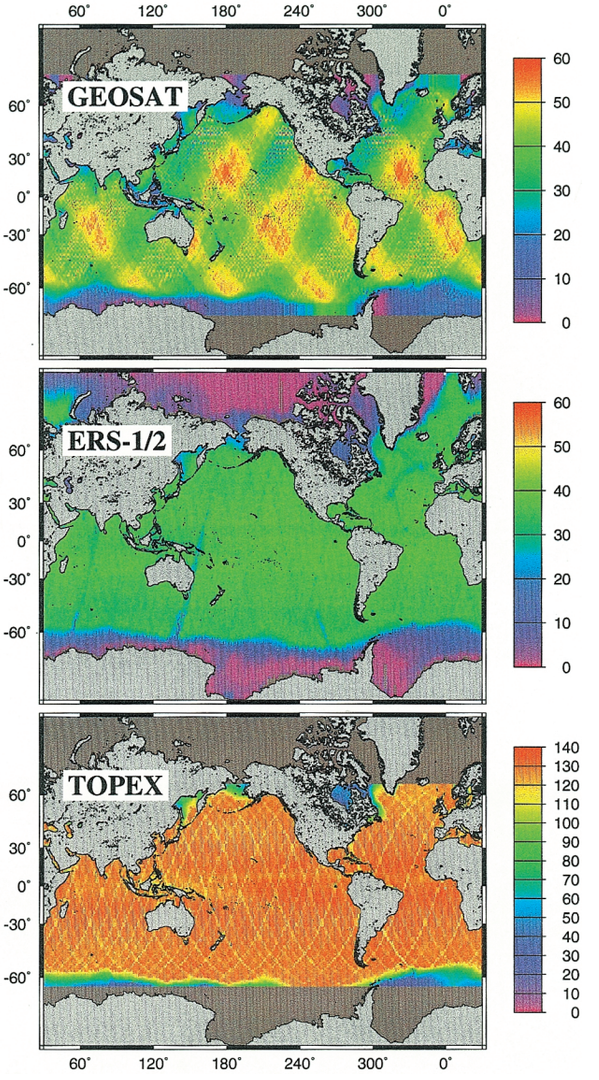

FIG. 1. Number of cycles stacked varies geographically for each satellite. Geosat, 62 possible cycles; ERS-1/2, 43 possible cycles; TOPEX, 142 possible cycles. The power of the noise falls off approximately linearly with the number of cycles stacked.

An example of combining data is presented for the Caspian Sea (Figure 2). Repeat satellite ground tracks for the three satellite orbits are shown. The grid of residual gravity illustrates where the profiles add information. The residual grid shows the short-wavelength information captured by the stacked altimeter profiles. At this map scale it is difficult to identify new features along the repeat tracks. However, we expect that the gain in resolution will become apparent when these data are combined with other gravity measurements or examined as individual profiles.

GROUND TRUTHING ERS DATA IN THE GULF OF MEXICO

We measure the improved accuracy and short-wavelength resolution of stacked ERS-1/2 profiles through comparison with high-accuracy marine gravity archives for the Gulf of Mexico from EDCON Inc. (Yale et al., 1998). EDCON's gravity field derives from shipboard gravity collected with a survey line spacing of 1 mile. When compared to satellite-derived gravity maps, EDCON's data represent the true gravity field. We extracted the ground-truth gravity along 40 stacked ERS-1/2 profiles (Figure 3). This is a region where the new gravity profiles will likely show the most improvement because the area is shallow.

Comparison plots between stacked profiles and ship profiles are presented in Figures 4 and 5 for all 40 profiles indicated in Figure 3. Thick lines show ship profiles, and thin lines show stacked profiles. Stacked profiles capture much of the structure resolved by the shipboard gravity, especially at wavelengths >50 km. Figure 6 enlarges two profiles to illustrate how stacked profiles improve short-wavelength resolution over the V7.2 grid. There is good agreement for some of the smaller scale features but poor agreement for others. A 10-km low-pass filter does not suppress all of the altimeter noise, but a 20-km filter may be too strong in shallow areas. Stacked profiles improve short-wavelength resolution because they are an average of 43 cycles versus 16 cycles for V7.2. To quantitatively assess the accuracy and resolution of the stacked gravity profiles, we perform two types of comparisons—an rms difference and a cross spectral analysis.

We computed the rms difference between the V7.2 profiles and the ship profiles and between the stacked profiles and the ship profiles (see Table 1). On average, the rms difference between stacked profiles and ship data (3.77 mGal)

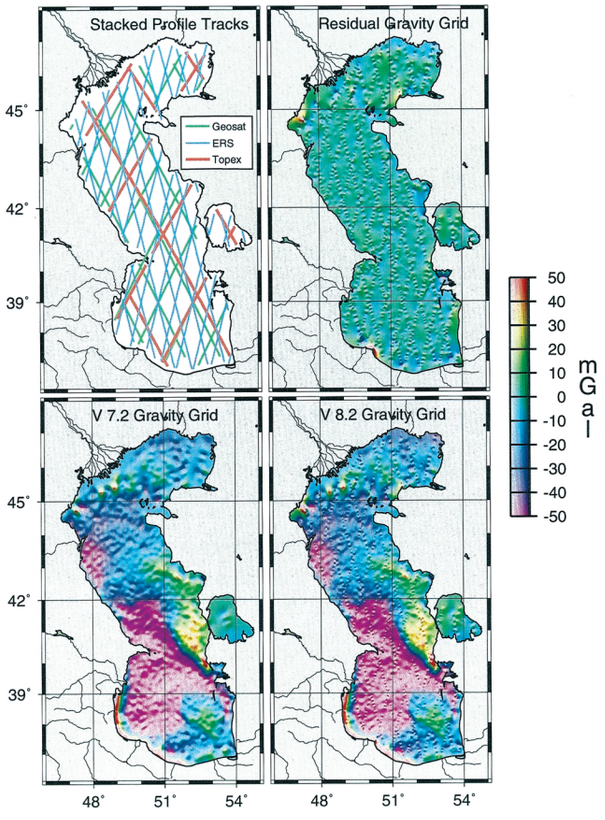

FIG. 2. We merge stacked gravity profiles with the V7.2 grid, creating a V8.2 gravity grid. Differencing stacked profiles from the V7.2 grid yields residual profiles. Gridding combines residual gravity profiles from all satellites. Adding the residual grid to the V7.2 grid produces the V8.2 grid.

Table 1. Difference between satellite and shipboard gravity for the Gulf of Mexico. See Figure 3 for profile locations.

	Ship, V7.2		Ship, Stacked Profiles	
Profile	Mean (mGal)	rms (mGal)	Mean (mGal)	rms (mGal)
A1	−6.25	2.95	−6.08	3.44
A2	−1.23	3.85	−2.01	4.18
A3	−2.64	3.85	−2.97	3.29
A4	−1.99	4.64	−1.44	4.64
A5	−1.79	3.66	−1.25	3.26
A6	−2.29	3.36	−2.11	2.70
A7	−1.92	3.57	−1.51	2.82
A8	−2.02	3.17	−2.44	3.06
A9	−3.11	4.73	−3.75	3.53
A10	−0.78	2.65	−0.97	2.97
A11	−0.19	4.79	−0.93	3.59
A12	0.36	4.99	0.12	5.24
A13	−1.23	4.48	−0.81	4.06
A14	0.67	5.65	0.88	5.41
A15	−0.38	4.36	−1.02	3.12
A16	−1.85	4.67	−2.33	4.63
A17	−2.12	4.62	−1.97	4.75
A18	−0.46	5.39	−0.40	4.02
A19	−2.61	3.43	−2.41	3.10
A20	−4.50	4.87	−4.04	4.45
D1	−1.94	4.90	−2.37	3.87
D2	−4.27	3.99	−4.23	3.25
D3	−2.38	3.16	−1.94	3.07
D4	0.62	6.44	−2.71	4.05
D5	−2.30	3.56	−2.48	2.88
D6	−0.42	3.20	−2.10	3.23
D7	−2.65	3.39	−3.07	3.94
D8	−0.99	3.54	−3.11	2.67
D9	0.06	6.02	−4.05	3.63
D10	−2.34	3.98	−3.54	3.48
D11	−1.16	3.67	−2.13	3.46
D12	−1.24	3.30	−0.80	3.36
D13	−1.21	4.55	−0.61	3.71
D14	−0.50	5.62	0.08	5.19
D15	−1.27	5.11	−2.12	4.36
D16	−2.68	5.63	−2.08	5.32
D17	−0.68	4.14	−1.11	4.60
D18	−2.45	3.51	−1.98	3.32
D19	−2.83	3.80	−2.82	3.57
D20	−3.60	3.11	−5.53	3.52
Mean	−1.76	4.21	−2.15	3.77
Min	−6.25	2.65	−6.08	2.67
Max	0.67	6.44	0.88	5.41

was lower than the rms difference between V7.2 and ship data (4.21 mGal). The rms difference between stacked profiles and ship data ranged from 2.67 to 5.41 mGal.

The spectral analyses compared stacked profiles to V7.2 and also stacked profiles to ship data. We estimated the spectral coherence between stacked profiles and V7.2 and between stacked profiles and ship data using Welch's method (1967) of estimating spectra by averaging over modified periodograms. For each of the three data sets (stacked profiles, V7.2 profiles, ship profiles), individual ascending and descending profiles were truncated to 256 point segments. All 256 point segments were Hanning windowed and then concatenated, producing three time series—one each for stacked profiles, V7.2 profiles, and ship profiles. The three full time series were used in spectral estimation. Profiles shorter than 256 points were excluded.

The results of our coherence estimate are presented in Figure 7. If we use the 0.5 coherence as a measure of resolution, stacked ERS-1/2 profiles resolve wavelengths >24 km while V7.2 profiles resolve wavelengths >26 km. The coherence is particularly improved for the stacked profiles in the wavelength band from 24 to 50 km.

DISCUSSION

Our results in the Gulf of Mexico show significant improvement in the accuracy and resolution of ERS-1/2 stacked profiles. These results are consistent with estimates of altimetry accuracy and resolution obtained in other geographic areas. Sandwell and Smith (1997) show their V7.2 grid has an rms accuracy of 3 to 6 mGal, depending on the proximity to a stacked profile. This is consistent with an independent rms accuracy estimate (3–9 mGal) of the V7.2 grid performed by Marks (1996). Accuracy and resolution depend on a variety of factors, including typical sea state and proximity to land.

There are fundamental limitations on the resolution of satellite gravity (Yale et al., 1998). Ocean surface waves limit the pulse-to-pulse accuracy of the altimeter so that doubling accuracy requires four times more data. Resolution improvements depend on local signal characteristics. Since ERS-1/2 and Geosat data span 10 years, another 30 years of data would be needed to double accuracy. The ERS-1/2 have a noisy onboard tracker, and significant improvements (still less than a factor of two) can be made in ERS-1/2 resolution through waveform repicking (Laxon and McAdoo, 1994, 1997; Green et al., 1998). Repicking will not improve Geosat and Topex data because they do not suffer from the noise problems of the ERS-1/2 onboard tracker.

The best way to use stacked gravity profiles for exploration is to augment more accurate local surveys. Satellite-derived gravity can provide the big picture needed for local interpretation, especially in areas where large-scale tectonics have influenced basin development. Biegert and Millegan (1998) review ways that satellite gravity is reducing exploration and production

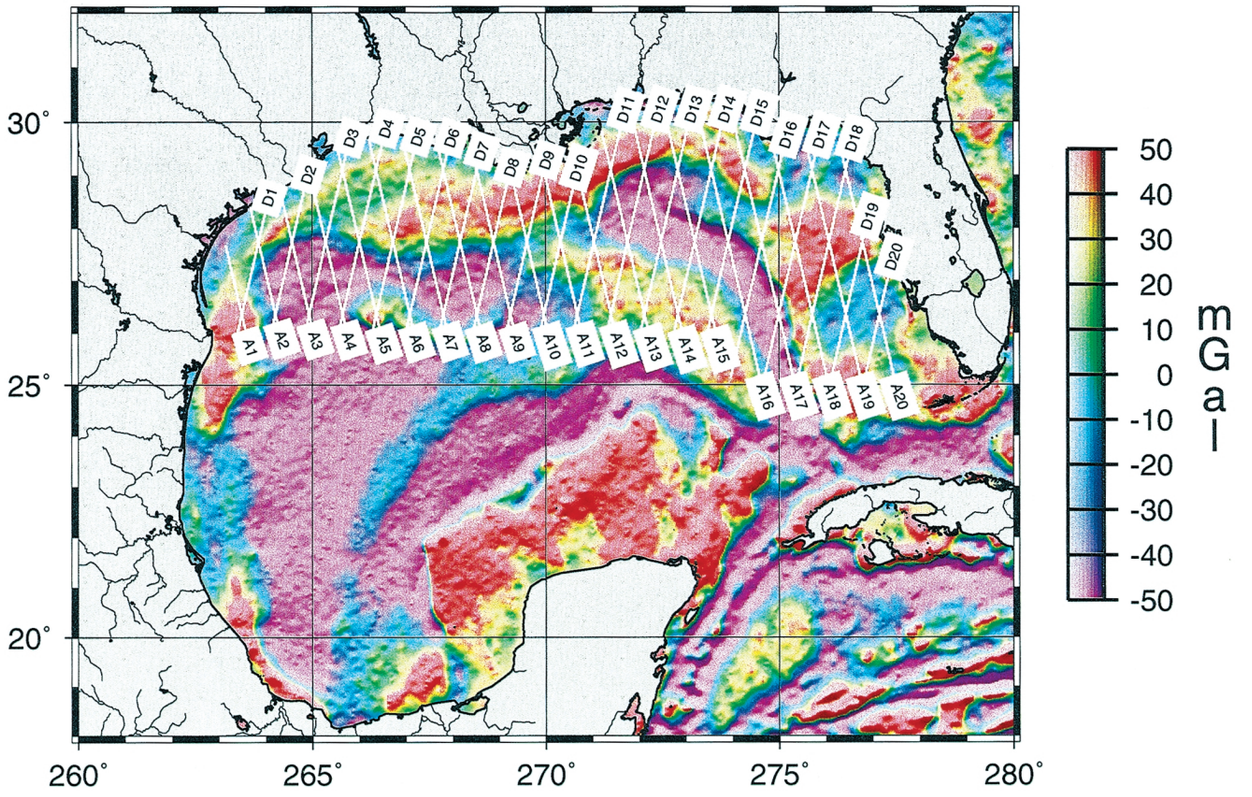

FIG. 3. Gulf of Mexico gravity grid created by combining stacked Geosat, ERS-1/2, and Topex data with Sandwell and Smith V7.2 gravity grid. The forty profiles labeled here are used to analyze the stacked ERS profiles versus V7.2 versus shipboard gravity. A1-A20 are ascending profiles. D1-D20 are descending profiles.

costs in the oil industry. For example, in Southeast Asia satellite gravity revealed previously undiscovered minibasins for the frontier exploration group, enabling them to relocate seismic lines for improved prospecting. In the deepwater Gulf of Mexico, drilling was suspended while Eddy Whopper passed the drill ship. An ocean circulation model constrained by satellite altimetry forecasted the path of the eddy, allowing drilling to resume without unnecessary damage or loss of time. And in the Black Sea, the only gravity data available comes from satellite altimetry which constrains geological interpretations and helps plan seismic surveys.

CONCLUSIONS

Iterating on the V7.2 grid with stacked profiles improves the recovery of short-wavelength gravity anomalies where stacked profiles are available. The best improvement from our new grid is likely to be in shallow regions where the upward continuation from the sea floor is minimized (Appendix A) and the shortest wavelength anomalies can be resolved at the sea surface.

A broad view of the gravity field over most of the world's oceans is available over the Internet (http://topex.ucsd.edu). Sedimentary basin locations and regional structures can be

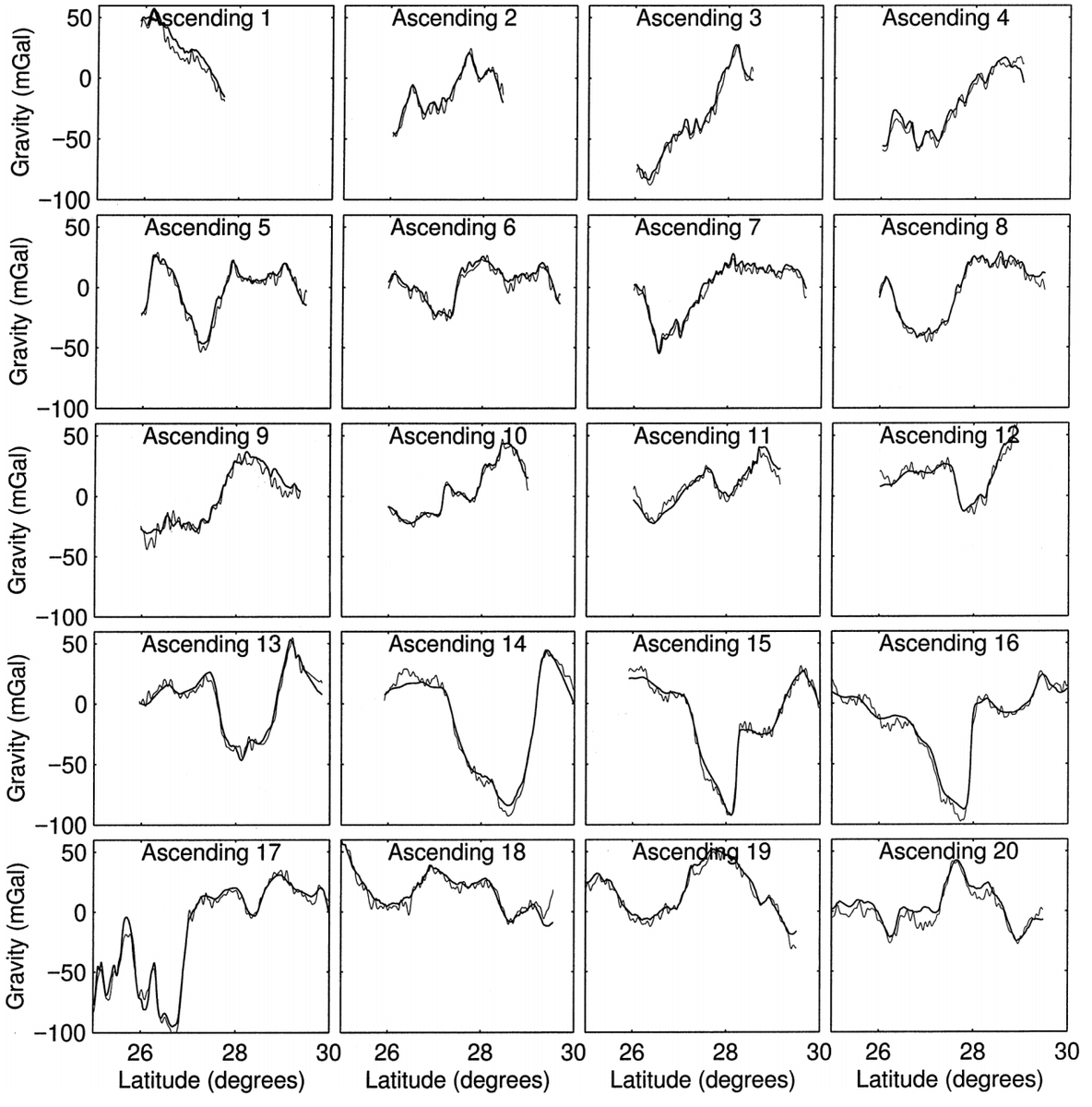

FIG. 4. Comparison of shipboard (thick lines) and stacked ERS-1/2 (thin lines) gravity in the Gulf of Mexico. See Figure 3 for profile (A1-A20) locations.

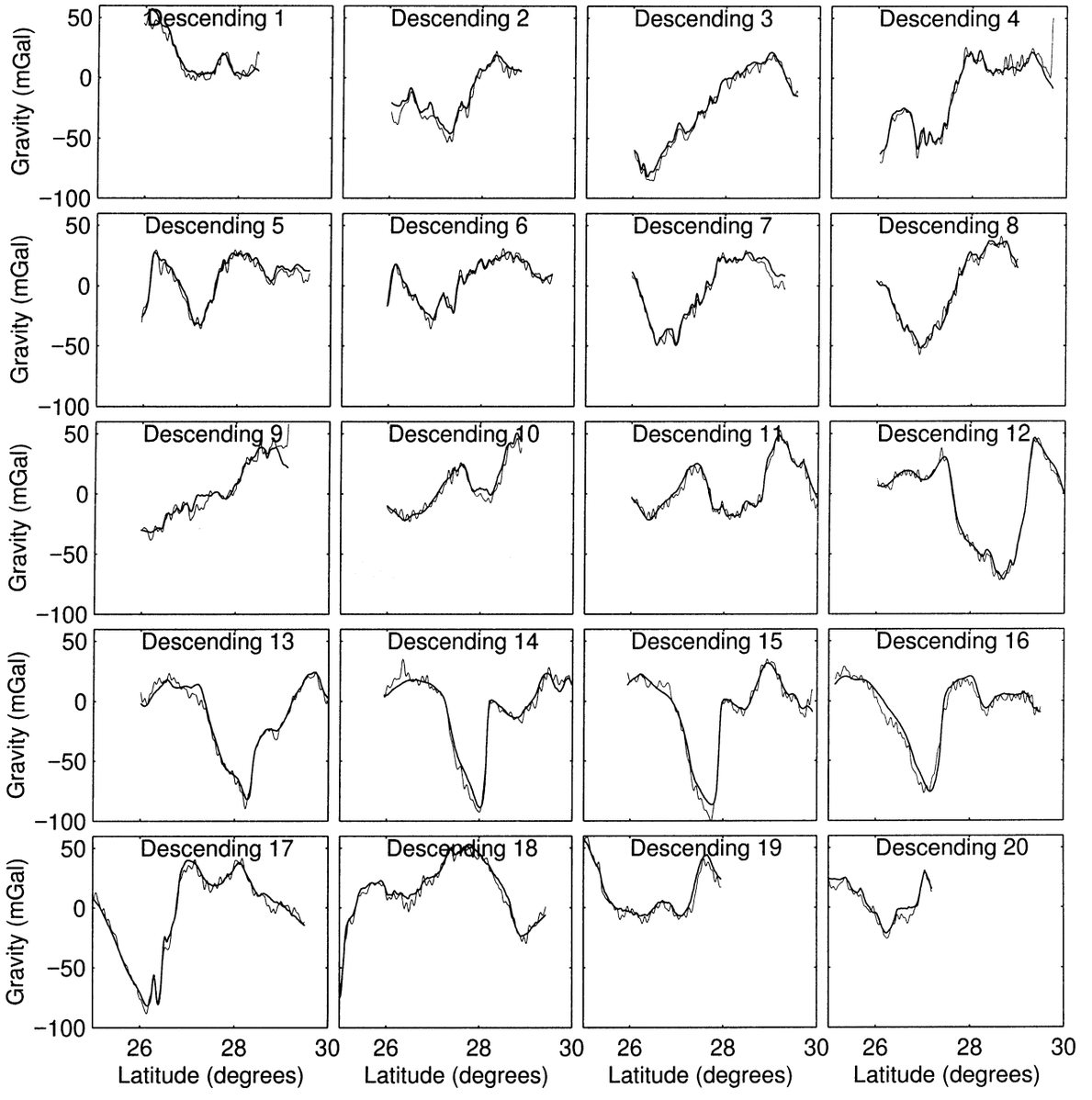

FIG. 5. Comparison of shipboard (thick lines) and stacked ERS-1/2 (thin lines) gravity in the Gulf of Mexico. See Figure 3 for profile (D1-D20) locations.

interpreted from satellite gravity. Satellite gravity provides regional control for detailed marine surveys. In fact, satellite gravity is usually more valuable and reliable than widely spaced public and commercial marine data acquired 20 or 30 years ago.

Our new stacked profiles and a recipe for combining them with other data are available over the Internet (http://topex.ucsd.edu).

ACKNOWLEDGMENTS

We thank Alan Herring and EDCON Inc. for providing the shipboard data used in this study. The ERS-1/2 data were provided by ESA through the French Processing and Archive Facility. Topex data were provided by AVISO, NASA, and CNES. We thank John Lillebridge for providing software to convert ERS-1/2 Altimeter Ocean Product data to NOAA-GDR data format. Remko Scharroo and Delft Institute for Earth-Oriented Space Research provided ERS-1/2 orbits. This paper benefited from reviews by Richard Hansen and Charles Campbell.

REFERENCES

Andersen, O. B., and Knudsen, P., 1998, Global marine gravity field from the ERS-1 and Geosat geodetic mission altimetry: J. Geophys. Res., **103**, 8129–8137.

Biegert, E. K., and Millegan, P. S., 1998, Beyond recon: The new world of gravity and magnetics: Leading Edge, **17**, 41–42.

Cazenave, A., Schaeffer, P., Berge, M., Brossier, C., Dominh, K., and Gennero, M. C., 1996, High-resolution mean sea surface

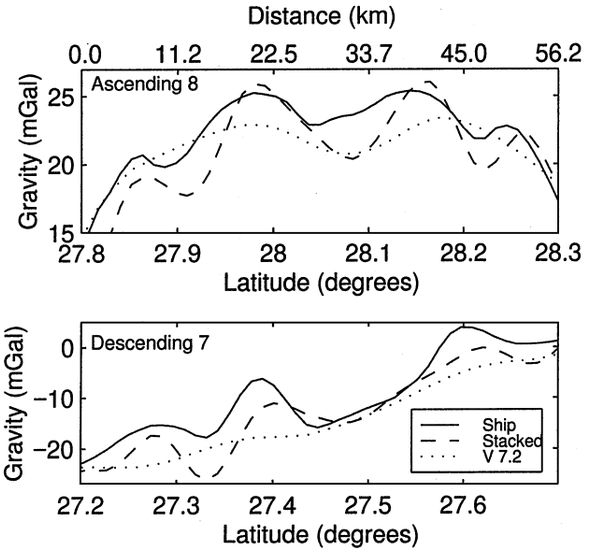

FIG. 6. Enlarged comparison between shipboard and satellite gravity for two profiles. The stacked profiles resolve shorter wavelengths than the V7.2 data. These stacked ERS-1/2 profiles contain up to 43 cycles of ERS-1/2 35-day-repeat data whereas V7.2 contains 16 cycles of 35-day-repeat ERS-1 data.

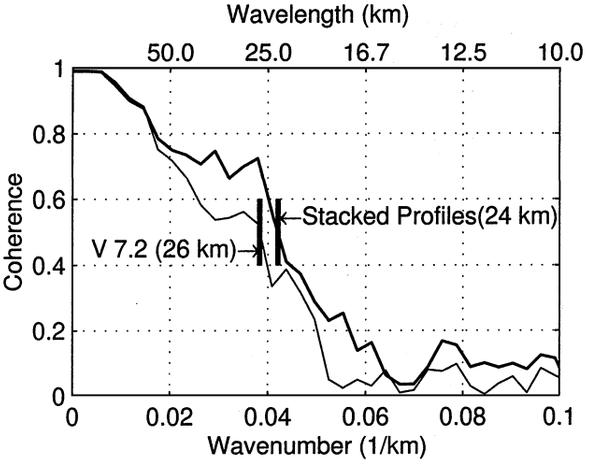

FIG. 7. Coherence between satellite and shipboard gravity. Stacked ERS-1/2 profiles resolve shorter wavelengths than the V7.2 grid, particularly in the band between 24 and 50-km wavelengths.

computed with altimeter data of ERS-1 (geodetic mission) and Topex-Poseidon: Geophys. J. Internat., **125**, 696–704.
Green, C. M., Fairhead, J. D., and Maus, S., 1998, Satellite-derived gravity: Where we are and what's next: Leading Edge, **17**, 77–79.
Haxby, W. F., Kramer, G. D., LaBrecque, J. L., and Weissel, J. K., 1983, Digital images of combined oceanic and continental data sets and their use in tectonic studies: EOS Trans. Amer. Geophys. Union, **64**, 995–1004.
Heiskanen, W. A., and Moritz, H., 1967, Physical geodesy: W. H. Freeman & Co.
Hwang, C., and Parsons, B., 1996, An optimal procedure for deriving marine gravity from multi-satellite altimetry: Geophys. J. Internat., **125**, 705–718.
Laxon, S., and McAdoo, D., 1994, Arctic ocean gravity field derived from ERS-1 satellite altimetry: Science, **265**, 621–624.
——— 1997, Antarctic Tectonics: Constraints from an ERS-1 satellite marine gravity field: Science, **276**, 556–560.
Marks, K. M., 1996, Resolution of the Scripps/NOAA marine gravity field from satellite altimetry: Geophys. Res. Lett., **23**, 2069–2072.
Nerem, R. S., et al., 1994, Gravity model development for the TOPEX/POSEIDON; Joint gravity models 1 and 2: J Geophys. Res., **99**, 24 421–24 447.
Rapp, R., and Yi, Y., 1997, Role of ocean variability and dynamic ocean topography in the recovery of the mean sea surface and gravity anomalies from satellite altimeter data: J. Geodesy, **71**, 617–629.
Rummel, R., and Haagmans, R. H. N., 1990, Gravity gradients from satellite altimetry: Marine Geodesy, **14**, 1–12.
Sandwell, D. T., and Smith, W. H. F., 1997, Marine gravity anomaly from Geosat and ERS-1 satellite altimetry: J. Geophys. Res., **102**, 10 039–10 054.
Scharroo, R., and Visser, P., 1998, Precise orbit determination and gravity field improvement for the ERS satellites: J. Geophys. Res., **103**, 8113–8127.
Small, C., and Sandwell, D. T., 1992, A comparison of satellite and shipboard gravity measurements in the Gulf of Mexico: Geophysics, **57**, 885–893.
Welch, P. D., 1967, The use of the fast Fourier transform for estimation of power spectra: A method based on time averaging over short modified periodograms: IEEE Trans. Audio Electroacoust., **AU15**, 70–73.
Yale, M. M., Sandwell, D. T., and Herring, A. T., 1998, What are the limitations of satellite altimetry?: Leading Edge, **17**, 73–76.
Yale, M. M., Sandwell, D. T., and Smith, W. H. F., 1995, Comparison of along-track resolution of stacked Geosat, ERS 1, and TOPEX satellite altimeters: J. Geophys. Res., **100**, 15 117–15 127.

APPENDIX A

ONE-DIMENSIONAL TRANSFORMATION METHOD

The geoid height $N(\mathbf{x})$, gravity anomaly $\Delta g(\mathbf{x})$, and other measurable quantities are related to the gravitational potential $\phi(\mathbf{x}, \mathbf{z})$ (Heiskanen and Moritz, 1967). We assume all of these quantities are deviations from a reference Earth model, so a flat Earth approximation can be used for the gravity computation [equation (A-11)]. In the following equations, the position $x = (x, y)$ and the wavenumber $\mathbf{k} = (k_x, k_y)$, where $k_x = 1/\lambda_x$ and λ_x is wavelength. To a first approximation, the geoid height is related to the gravitational potential by Brun's formula:

$$N(\mathbf{x}) \cong \frac{1}{g_0}\phi(\mathbf{x}, 0), \tag{A-1}$$

where g_0 is the average acceleration of gravity (9.81 ms^{-2}). The gravity anomaly is

$$\Delta g(\mathbf{x}) = -\frac{\partial \phi(\mathbf{x}, 0)}{\partial z}. \tag{A-2}$$

The east component of vertical deflection is

$$\eta(\mathbf{x}) \equiv -\frac{\partial N}{\partial x} \cong \frac{-1}{g_0}\frac{\partial \phi}{\partial x}. \tag{A-3}$$

The north component of vertical deflection is

$$\xi(\mathbf{x}) \equiv -\frac{\partial N}{\partial y} \cong \frac{-1}{g_0}\frac{\partial \phi}{\partial y}. \tag{A-4}$$

Laplace's equation relates these three partial derivatives of the gravitational potential:

$$\frac{\partial^2 \phi}{\partial x^2} + \frac{\partial^2 \phi}{\partial y^2} + \frac{\partial^2 \phi}{\partial z^2} = 0. \tag{A-5}$$

Substitution of equations (A-2), (A-3), and (A-4) into Laplace's equation (A-5) yields

$$\frac{\partial \Delta g}{\partial z} = -g_0\left[\frac{\partial \eta}{\partial x} + \frac{\partial \xi}{\partial y}\right]. \tag{A-6}$$

Vertical gravity gradient can be computed from grids of east and north vertical deflection (Rummel and Haagmans, 1990).

Following Haxby et al. (1993), the differential equation (A-6) reduces to an algebraic equation when Fourier transformed. The forward and inverse Fourier transforms are

$$F(\mathbf{k}) = \int_{-\infty}^{\infty}\int_{-\infty}^{\infty} f(\mathbf{x}) \exp[-i2\pi(\mathbf{k}\cdot\mathbf{x})]\, d^2\mathbf{x} \tag{A-7}$$

and

$$f(\mathbf{x}) = \int_{-\infty}^{\infty}\int_{-\infty}^{\infty} F(\mathbf{k}) \exp[i2\pi(\mathbf{k}\cdot\mathbf{x})]\, d^2\mathbf{k} \tag{A-8}$$

The Fourier transform of equation (A-6) is

$$\frac{\partial \Delta g(\mathbf{k}, z)}{\partial z} = -i2\pi g_0[k_x \eta(\mathbf{k}) + k_y \xi(\mathbf{k})]. \tag{A-9}$$

Solving Laplace's equation in the wavenumber domain yields the upward continuation formula, which relates the gravity anomaly at the earth's surface to the gravity anomaly at some elevation z:

$$\Delta g(\mathbf{k}, z) = \Delta g(\mathbf{k}, 0) \exp[-2\pi|\mathbf{k}|z], \tag{A-10}$$

where $|\mathbf{k}| = \sqrt{k_x^2 + k_y^2}$. Taking the derivative of equation (A-10) with respect to z and evaluating the result at $z = 0$ results in an algebraic formula relating the Fourier transforms of the gravity anomaly, east and north vertical deflection:

$$\Delta g(\mathbf{k}, 0) = \frac{ig_0}{|\mathbf{k}|}[k_x \eta(\mathbf{k}) + k_y \xi(\mathbf{k})] \tag{A-11}$$

When a dense network of satellite altimeter profiles is available, as for the V7.2 grid, we construct grids of east η and north ξ vertical deflection and operates on these grids in 2-D Fourier transform domain. Since all of the stacked repeat profile data have a sparse track spacing, a 1-D approximation is used to maintain all along-track resolution. We subtract the V7.2 vertical deflection from stacked vertical deflection profiles and then apply the 1-D transformation to the residual vertical deflection profiles.

First we align the x-axis of the local coordinate system with the satellite ground track. Then we assume that the curvature of the residual geoid in the crosstrack direction is zero, eliminating the y-derivatives in equations (A-5) and (A-6) and the k_y terms in equations (A-9) and (A-11). After simplifying, the Fourier transform of the along-track gravity anomaly is related to the Fourier transform of the along-track vertical deflection:

$$\Delta g(k_x) = \frac{ig_0 k_x}{|k_x|}\eta(\mathbf{k}). \tag{A-12}$$

This procedure of Fourier transforming the along-track vertical deflection, multiplying by $ig_0\text{sgn}(k_x)$, and inverse Fourier transforming corresponds to Hilbert transforming the vertical deflection profile and multiplying by g_0. After converting residual vertical deflection profiles into residual gravity profiles using equation (A-12), we add residual gravity profiles to the V7.2 gravity grid.